PROCEEDINGS A

royalsocietypublishing.org/journal/rspa

Research

Cite this article: van de Velde SJ, Hylén A, Eriksson M, James RK, Kononets MY, Robertson EK, Hall POJ. 2023 Exceptionally high respiration rates in the reactive surface layer of sediments underlying oxygen-deficient bottom waters. *Proc. R. Soc. A* **479**: 20230189. https://doi.org/10.1098/rspa.2023.0189

Received: 20 March 2023
Accepted: 15 June 2023

Subject Areas:
geochemistry, biogeochemistry

Keywords:
marine sediment, carbon cycle, geochemistry

Author for correspondence:
Sebastiaan J. van de Velde
e-mail: svandevelde@naturalsciences.be

Exceptionally high respiration rates in the reactive surface layer of sediments underlying oxygen-deficient bottom waters

Sebastiaan J. van de Velde[1,2,†], Astrid Hylén[3], Mats Eriksson[4], Rebecca K. James[2], Mikhail Y. Kononets[1,5], Elizabeth K. Robertson[5] and Per O. J. Hall[5]

[1]Operational Directorate Natural Environment, Royal Belgian Institute of Natural Sciences, 1000 Brussels, Belgium
[2]Department of Geoscience, Environment and Society, Université Libre de Bruxelles, 1050 Brussels, Belgium
[3]Department of Biology, University of Antwerp, 2610 Wilrijk, Belgium
[4]Department of Health, Medicine and Caring Sciences, Linköping University, 581 83 Linköping, Sweden
[5]Department of Marine Sciences, University of Gothenburg, 405 30 Gothenburg, Sweden

SJvdV, 0000-0001-9999-5586; RKJ, 0000-0002-3679-8531

Organic carbon (OC) burial efficiency, which relates the OC burial rate to respiration in the seafloor, is a critical parameter in the reconstruction of past marine primary productivities. The current accepted theory is that sediments underlying oxygen-deficient (anoxic) bottom waters have low respiration rates and high OC burial efficiencies. By combining novel *in situ* measurements in anoxic basins with reaction-transport modelling, we demonstrate that sediments underlying anoxic bottom waters have much higher respiration rates than commonly assumed. A major proportion of the carbon respiration is concentrated in the top millimeter—the so-called 'reactive surface layer'—which is likely a feature in approximately 15% of the coastal seafloor. When re-evaluating previously published data in light of our results, we conclude that the impact of bottom-water anoxia on

[†]Present address: Department of Biology, University of Antwerp, Antwerp, Belgium.

Electronic supplementary material is available online at https://doi.org/10.6084/m9.figshare.c.6729334.

THE ROYAL SOCIETY PUBLISHING

OC burial efficiencies in marine sediments is small. Consequently, reconstructions of past marine primary productivity in a predominantly anoxic ocean based on OC burial rates might be underestimated by up to an order of magnitude.

1. Introduction

The balance between organic carbon (OC) respiration and burial in marine sediments regulates the atmospheric concentrations of oxygen (O_2) and carbon dioxide (CO_2) on geological time scales [1]. The OC burial efficiency, the fraction of OC arriving at the sediment surface that is buried, is determined by the rate at which OC is respired. The respiration rate is in turn controlled by factors intrinsic to the OC material, such as type and age, and physical or biogeochemical environmental conditions [2,3].

Exposure to oxygenated water is seen as one of the most important biogeochemical factors regulating the OC burial efficiency, as it is believed to stimulate OC respiration [4–6]. A compilation of OC burial efficiencies suggests that sediments deposited in oxic bottom waters can have OC burial efficiencies that are 10 s of per cent lower than sediments deposited in anoxic bottom waters and that the difference becomes negligible at sedimentation rates above $200\,g\,m^{-2}\,yr^{-1}$ [4,7]. A lower OC burial efficiency with increased O_2 exposure is supported by both field observations [6] and theoretical arguments [8]. Experimental studies have demonstrated that some fractions of organic matter are degraded less efficiently under anoxic conditions [9–11]. This observation is in line with thermodynamic arguments that certain OC compounds only yield enough energy to support microbial growth if they are coupled to the reduction of O_2 [12] and that some OC bonds only can be broken by oxygenase enzymes that require O_2 as substrate [13]. Additionally, sediments underlying oxic bottom waters typically host a variety of benthic fauna, which contribute to the processing of OC and potentially stimulate respiration [14,15].

The extent to which O_2 exposure decreases the OC burial efficiency under natural conditions is however poorly constrained. Oxygen-deficient waters only cover less than 0.5% of the present-day seafloor [16], and OC burial efficiencies have only been determined for a handful of sites [5]. Moreover, the field data available from oxygen-deficient sites are based on different methodologies than field data from oxygenated sites, which causes comparability issues. In sediments underlying oxygenated bottom waters, OC respiration rates are typically derived from chamber incubations measuring total O_2 uptake, or from high-resolution (micrometre scale) O_2 profiles measured with microsensors [17,18]. In sediments underlying hypoxic bottom waters ($0\,\mu M < [O_2] < 63\,\mu M$), OC respiration rates are often derived from fluxes of dissolved inorganic carbon (DIC) [19,20]. By contrast, respiration rates in sediments underlying anoxic bottom waters have been derived mainly from vertical sediment core profiles at centimetre-scale resolution [17]. However, this method is generally unable to resolve small-scale biogeochemical processes at the sediment–water interface (SWI) that result in steep chemical gradients [21,22]. The presence of such gradients implies that the respiration rate is higher near the SWI resulting in a 'reactive surface layer'. Methods that are unable to resolve the reactive surface layer would underestimate the OC respiration rate, and thus overestimate the OC burial efficiency in sediments underlying anoxic bottom waters.

To test our reactive surface layer hypothesis, we visited nine field sites along two depth transects in two archetypical long-term anoxic basins (the eastern and western Gotland Basins (EGB and WGB), central Baltic Sea). We estimated OC respiration rates and burial efficiencies by deploying autonomous benthic chamber landers to measure DIC fluxes and compared these with several core-based methods; sulphate reduction rates (SRRs) from ^{35}S whole-core incubations, and inverse diagenetic modelling of vertical DIC, dissolved sulphate (SO_4^{2-}) and particulate OC (POC) sediment profiles, together with measurements of mass accumulation rates (MARs).

2. Materials and methods

(a) Field site

The EGB and WGB are situated in the central part of the Baltic Sea (figure 1). The maximum water depths are 249 m and 459 m in the EGB and WGB, respectively. Both basins have a strong and permanent halocline at approximately 60–80 m depth. A combination of eutrophication and stratification has led to prolonged periods of anoxia ($[O_2] < 0.5\,\mu M$) below the halocline. The sediments above the halocline (less than 80 m depth) are strongly affected by waves and bottom currents and are generally classified as erosion-transport bottoms. These shallow sediments show no net long-term sediment accumulation and consist of coarser material since finer material is rapidly eroded and transported to the deeper basin [23–25].

(b) Benthic lander deployments

Benthic chamber landers were deployed twice per location during each campaign, with a few exceptions due to ship time scheduling or weather constraints. Before each lander deployment, water-column profiles of temperature, salinity and oxygen were recorded using a CTD instrument (SBE 911, Sea-Bird Scientific) equipped with a high-accuracy O_2 sensor (SBE 43, Sea-Bird Scientific). The lander deployment procedure is detailed in [26,27]. Before the incubation, the lander frame was left hanging for 2 h at a depth of approximately 1 m above the seafloor with open chambers that were stirred. The frame was then slowly lowered onto the seafloor, and the chambers were inserted in the sediment. The chamber lids were left open for another 2 h with continuous stirring. Sediment and water were incubated for 37 h at station EGB-1 and 14 h at all other stations. After lander recovery, syringe samples were immediately filtered in thoroughly pre-rinsed cellulose acetate filters (Sartorius, 0.45 mm pore size) and were stored at 4°C until analysis within 24 h.

Benthic fluxes of DIC were calculated from the concentration change in the chamber water over time. Concentrations were corrected for the small dilution that took place when new bottom water entered the chamber during syringe sampling. Data points were first screened for outliers and leverage points, and subsequently, a least-square regression line was fitted to concentration data versus time. The data evaluation procedure is outlined in [28].

(c) Sediment sampling

In 2018, sediment was retrieved using a multiple corer (9.9 cm inner diameter) or a modified box corer [29]. In 2021, sediment was retrieved using a GEMAX gravity corer (9 cm inner diameter). Sample processing started immediately after sample collection. Two cores for POC and DIC measurements were sliced in the open air at 0.5 cm resolution from 0 to 2 cm depth, at 1 cm resolution between 2 and 6 cm depth, and in 2 cm slices from 6 to 20 cm depth. Not all collected cores (notably in WGB-1 and EGB-1) reached 20 cm depth. Samples for POC were frozen until further processing, while sediment sections for DIC analysis (only collected in 2021) were collected in 50 ml centrifuge tubes (polypropylene; VWR) whereafter porewater was extracted by centrifugation at 2500 g for 10 min (Beckman-Coulter Allegra X-30 series, Switzerland) and subsequent filtration through 0.45 µm pore size cellulose acetate filters (Sartorius, Minisart). Two cores were sectioned under an N_2 atmosphere in a portable glove bag (Captair Pyramid, Erlab, France) at the same resolution as above for porewater SO_4^{2-} samples. In the glove bag, the sediment sections were collected in 50 ml centrifuge tubes into which Rhizons samplers (pore size approximately 0.15 mm; Rhizosphere Research Products, The Netherlands) were inserted until the porous part was completely covered. Syringes attached to the Rhizons were drawn back and fixed in this position, creating a vacuum which extracted the porewater. Porewater samples for sulphate analysis were stabilized using ZnAc solution (2.25 ml of a 10% ZnAc solution per 0.25 ml sample) and stored at 4°C; porewater samples for DIC analysis were stored at 4°C and

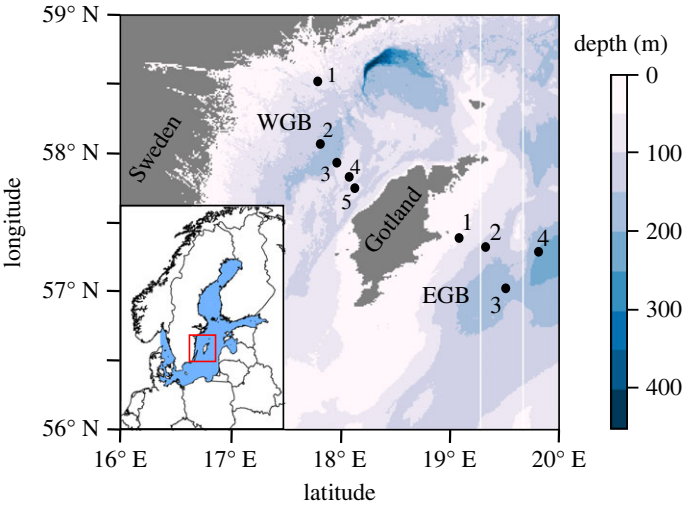

Figure 1. Bathymetry map of the EGB and WGB with the locations of the sampling stations. Bathymetry is retrieved from https://portal.emodnet-bathymetry.eu/?menu=19#.

analysed within 24 h. In 2021, one core per station was collected for ^{210}Pb dating at the University of Linköping, while ^{210}Pb-dating data for the EGB stations were taken from [24]. Three (2018) or two (2021) subcores (2.5 cm inner diameter) were collected from each station from the box corer or GEMAX corer for ^{35}S SRR measurements.

(d) Sediment porosity

Sediment–water content was calculated from the weight difference before and after freeze-drying of the sediment samples. The solid-phase density for EGB sediments was determined previously to be 1.4 g cm^{-3} [28] and the density of WGB sediments was assumed to be identical. Sediment porosity (volume of pore water per volume of bulk sediment) was calculated from sediment–water content and solid-phase density.

(e) Sediment dating

The determination of the sediment MAR is based on the two ^{210}Pb-dating methods: constant flux constant sedimentation and constant rate of supply (CRS) [30,31]. The determination of ^{210}Pb was done through its progeny ^{210}Po. About 0.5 g of sediment from each sediment layer was used for the determination of^{210}Po. After sample dissolution using the microwave digestion method, polonium was self-deposited from weak HCl solution onto silver disc [32–34]. As chemical yield determinate, ^{209}Po was used. The Po discs were measured by alpha spectrometry between 1 and 2 days. To determine the support level of ^{210}Pb, the determination of ^{226}Ra concentration was evaluated as the weighted mean activity concentration of the daughters (^{214}Pb and ^{214}Bi). The samples were put in radon-tight vacuum-sealed containers and left for three weeks, ensuring secular equilibrium between ^{226}Ra and its progenies and no radon from the sample containers [35]. The vacuum-sealed sample was then measured in a calibrate geometry on a high-purity gamma detector (HPGe) for 2–3 days.

(f) Sulphate reduction rates

SRRs in the sediment were determined with the ^{35}S radiotracer method [36]. Overlying water was removed from the sediment core and 5 µl of radiotracer was injected at 1 cm depth increments for

approximately 10 cm to reach a total activity of 60 kBq per depth horizon. The cores were wrapped in aluminium foil and were then placed in a cold room at *in situ* temperature for approximately 12 h. The incubation was halted by slicing the cores at 1 cm intervals and collecting the sediment layers into 50 ml plastic centrifuge tubes filled with 20 ml zinc acetate (20% w/w). Samples were kept frozen at −20°C until analysis using the hot chromium distillation method [37]. SRRs are reported per volume sediment (nmol S cm^{-3} d^{-1}).

(g) Geochemical analyses

DIC concentrations in the lander samples from 2018 and porewater samples from 2021 were determined onboard the ship by non-dispersive infrared spectrometry (LI-COR 6262) after acidification with phosphoric acid [24]. A two-point calibration and correction for potential drift in the system were obtained by repeated measurements of certified reference material (Dickson Laboratory, Scripps Inst. of Oceanography). The analytical precision was 0.6% (relative standard deviation). In 2021, DIC concentrations in lander samples were measured onboard using the same principle using an Apollo AS-C5 (Apollo SciTech) with a precision of 0.4% (relative s.d.).

Samples for SO_4^{2-} analysis were diluted 10 times and separated by ion chromatography using an isocratic eluent (3.5 mM Na_2CO_3/1 mM $NaHCO_3$) combined with Dionex AS-14 analytical column (Thermo Scientific). Quantification was done by a conductivity detector (ED40 electrochemical detector) [38] with an analytical precision of 8%.

Freeze-dried samples were analysed for POC by elemental analysis isotope ratio mass spectrometry (Sercon). Samples were exposed to acid fumes of 37% HCl for 48 h to remove the inorganic carbon. The POC values are expressed as mass % of the dry weight of the sediment sample. The precision was less than 5% for the POC measurements.

(h) Rate estimations

The burial efficiency of OC was calculated as the ratio between the OC burial flux (J_{OC}^{burial}) and the OC input flux (J_{in}^{OC}). The latter was calculated as the sum of the OC burial flux and integrated respiration rate (R_{min}^{int}):

$$BE(\%) = 100\frac{J_{burial}^{OC}}{J_{in}^{OC}} = 100\frac{J_{burial}^{OC}}{J_{burial}^{OC} + R_{min}^{int}}. \tag{2.1}$$

The burial flux of OC (J_{OC}^{burial}) was calculated based on the sedimentation flux (J_S, or MAR; in g m^{-2} d^{-1}) and the concentration of OC at the bottom of the sediment column (C_{bottom}^{OC}; in dry wt %), and converted to mmol C m^{-2} d^{-1}:

$$J_{burial}^{OC} = \frac{J_S C_{bottom}^{OC}}{12} 10^{-2} 10^{3}. \tag{2.2}$$

The integrated respiration rate R_{min}^{int} was estimated via a lander-based method, i.e. the *in situ* measured DIC flux, and via four different core-based methods, based on the (i) vertical POC profile, (ii) porewater DIC profile, (iii) porewater SO_4^{2-} profile and (iv) ^{35}S radiotracer method.

The lander-derived DIC flux was assumed to be entirely generated by the respiration of OC, which is a valid assumption in these sediments, given there are no carbonate minerals or significant deep sources of DIC (e.g. methane hydrates) [24]. The integrated respiration rate can then be estimated as

$$R_{min}^{int} = J_{up}^{DIC}. \tag{2.3}$$

Except for stations EGB-1 and WGB-1, our field sites were unbioturbated, which means solid-phase transport is only governed by the downward advection of accumulating sediment. If we assume that the OC concentration in the top layer is representative of the sediment surface and

the sediment is in a steady state, the integrated respiration rate in the whole sediment interval can be calculated as

$$R_{\text{min}}^{\text{int}} = J_{\text{input}}^{\text{OC}} - J_{\text{burial}}^{\text{OC}} = J_S \frac{C_{\text{top}}^{\text{OC}} - C_{\text{bottom}}^{\text{OC}}}{12} 10^{-2} 10^{3}. \tag{2.4}$$

Alternatively, since there are no other sources of DIC in the sediment, the integrated respiration rate can be estimated from the integrated DIC production ($R_{\text{prod}}^{\text{DIC}}$) in the sediment.

$$R_{\text{min}}^{\text{int}} = J_{\text{prod}}^{\text{DIC}}. \tag{2.5}$$

Our field sites were almost entirely anoxic (aside from EGB-1), contain negligible amounts of reactive iron oxides [28], and SO_4^{2-} does not become depleted. Under these conditions, organic matter respiration is almost entirely driven by sulphate reduction [39]. Hence, the integrated respiration rate can be estimated from the integrated sulphate production ($R_{\text{prod}}^{\text{SO}_4^{2-}}$) as follows

$$R_{\text{min}}^{\text{int}} = 2R_{\text{prod}}^{\text{SO}_4^{2-}}, \tag{2.6}$$

where the two accounts for the stoichiometric ratio of carbon versus sulfur during sulphate reduction, and the negative sign is because SO_4^{2-} is consumed as OC is respired. The production rates $R_{\text{prod}}^{\text{DIC}}$ and $R_{\text{prod}}^{\text{SO}_4^{2-}}$ were calculated by inversely fitting a diagenetic model to the measured porewater profile using the R-script FLIPPER [40], which follows a similar procedure as outlined in [41]. FLIPPER analysis results are shown in the electronic supplementary material, figures S3 and S4. Finally, we measured sulphate reduction directly using the ^{35}S isotope method [36]. Based on this measurement, the integrated respiration rate can be calculated as follows:

$$R_{\text{min}}^{\text{int}} = 2 \sum_{\text{top}}^{\text{bottom}} \text{SRR}(x) \Delta x. \tag{2.7}$$

(i) Reaction-transport models

To test the impact of diffusive boundary layer (DBL) erosion on the benthic DIC flux measured using the benthic chamber lander, we designed a one-dimensional reaction-transport model for DIC, which was calibrated to the deepest station of the WGB (WGB-2). The model is described in detail in the electronic supplementary material, information, section S1. In short, a fixed rate of OC respiration was applied and transport of DIC only happened via diffusion and advection. The model was run to a steady state with four different DBL thicknesses (0.2 – 0.5 mm – 1.0 – 2.0 mm). Afterwards, the DBL was removed and the benthic DIC flux was simulated for 10 h.

To test the hypothesis of the reactive layer, we designed a one-dimensional reaction-transport model that simulated the coupled C-S cycle. The model is described in detail in the electronic supplementary material, section S2. In short, the model comprised five state variables (less reactive and highly reactive POC, DIC, dissolved sulphate and dissolved sulfide) and two reactions (respiration of less reactive POC coupled to sulphate reduction and respiration of highly reactive POC coupled to sulphate reduction). The model was calibrated for the field site with the largest difference between lander-based and core-based respiration rate estimates, and for which we had the most complete dataset (WGB-5). The model was run to a steady state with only less reactive POC (amount and reactivity calibrated to the field data), and with the addition of 20, 40 and 60 mmol C m^{-2} d^{-1} of highly reactive POC.

3. Results

Four stations were sampled in the EGB in April 2018, and five stations in the WGB in August 2021 (figure 1 and table 1). The number of datapoints per site is limited, yet the observed patterns are consistent among all visited field sites, which indicates our results are robust. Station EGB-1 is the shallowest and underlies a fully oxygenated water column. EGB-1 is categorized as an 'erosion-transport' bottom, meaning that there is very little long-term accumulation of sediment [23,28]. The other EGB stations are long-term anoxic accumulation sediments at increasing water

Table 1. Field site characteristics at the time of sampling. Bottom water salinity, temperature and oxygen concentrations were measured using CTD and with sensors on the benthic landers. Range of estimated MARs per site, determined with the CRS method (see methods for details). For calculations, the mean MAR is used. BW, bottom water; SRR, sulphate reduction rate; MAR, mass accumulation rate; DIC, dissolved inorganic carbon.

station	coord.	year	water depth (m)	sal. —	temp. (°C)	$[O_2]_{BW}$ (µM)	MAR (g m^{-2} yr^{-1})	SRR (mmol S m^{-2} d^{-1})	DIC flux[a] (mmol C m^{-2} d^{-1})
EGB-1	N 57°23′ E 19°05′	2018	60	7.5	3.0	~355	n/a[b]	0.7 – 1.8	8 – 16
EGB-2	N 57°20′ E 19°19′	2018	130	12	6.7	anoxic	29–136	3.3 – 5.1	14 – 30
EGB-3	N 57°02′ E 19°30′	2018	170	13	6.9	anoxic	51–150	4.7 – 7.6	37 – 56
EGB-4	N 57°17′ E 19°48′	2018	210	13	6.9	anoxic	79–94	5.1 – 5.9	19 – 68 (127)
WGB-1	N 58°31′ E 17°48′	2021	75	10	5.7	0–20	108–285	1.3	6
WGB-2	N 58°04′ E 17°49′	2021	170	11	6.3	anoxic	59 – 285	4.8 – 7.3	14 – 36 (143)
WGB-3	N 57°56′ E 17°58′	2021	160	11	6.2	anoxic	84–226	2.3 – 2.6	8 – 75
WGB-4	N 57°50′ E 18°05′	2021	100	11	6.2	anoxic	70–230	0.8 – 2.0	18 – 38
WGB-5	N 57°45′ E 18°08′	2021	110	11	6.1	anoxic	60–180	0.9 – 1.2	23 – 72

[a]Values between brackets are outliers.

[b]The MAR for station EGB-1 is highly uncertain, because regular erosion occurs at this site, leading to high amounts of sediment removal from the seafloor (see [23] for a more detailed discussion).

depth from EGB-2 to EGB-4. The bottom water at station WGB-1 is hypoxic, while the other WGB stations are long-term anoxic (table 1). At each station, we deployed the autonomous Gothenburg benthic chamber landers [26] to measure sediment–water fluxes of DIC. We further collected sediment cores to determine the vertical profiles of POC, DIC and SO_4^{2-}, estimated the SRR using ^{35}S tracers [36], and determined the MAR through ^{210}Pb-dating.

The POC concentrations at the shallow station EGB-1 are low (less than 1 wt%; figure 2*a*), consistent with the erosion of finer silt particles with which OC is associated [23,24]. The sediment at the deeper stations contains more POC, up to 20 wt% near the SWI at the deepest station (EGB-4; figure 2*a*). The trend of increasing sediment POC content with water depth is a consequence of constant particle shuttling, which transfers silt and organic matter to the deeper parts of the Baltic Sea subbasins [23]. The porewater concentrations of SO_4^{2-} and estimated SRR indicated that the sedimentary OC respiration also increases with water depth (figure 2*c*,*d*). At station EGB-1, there is no trend in the porewater SO_4^{2-} profile and the SRR decreases rapidly with sediment depth. By contrast, at the deeper EGB stations, SO_4^{2-} concentrations show a clear decrease with sediment depth, and SRRs remain high in the upper 5–10 cm of the sediment, corresponding to the sediment layer with elevated POC concentrations (figure 2*a*,*d*). The trend of increasing OC respiration rates is confirmed by the *in situ* benthic DIC fluxes, which increase

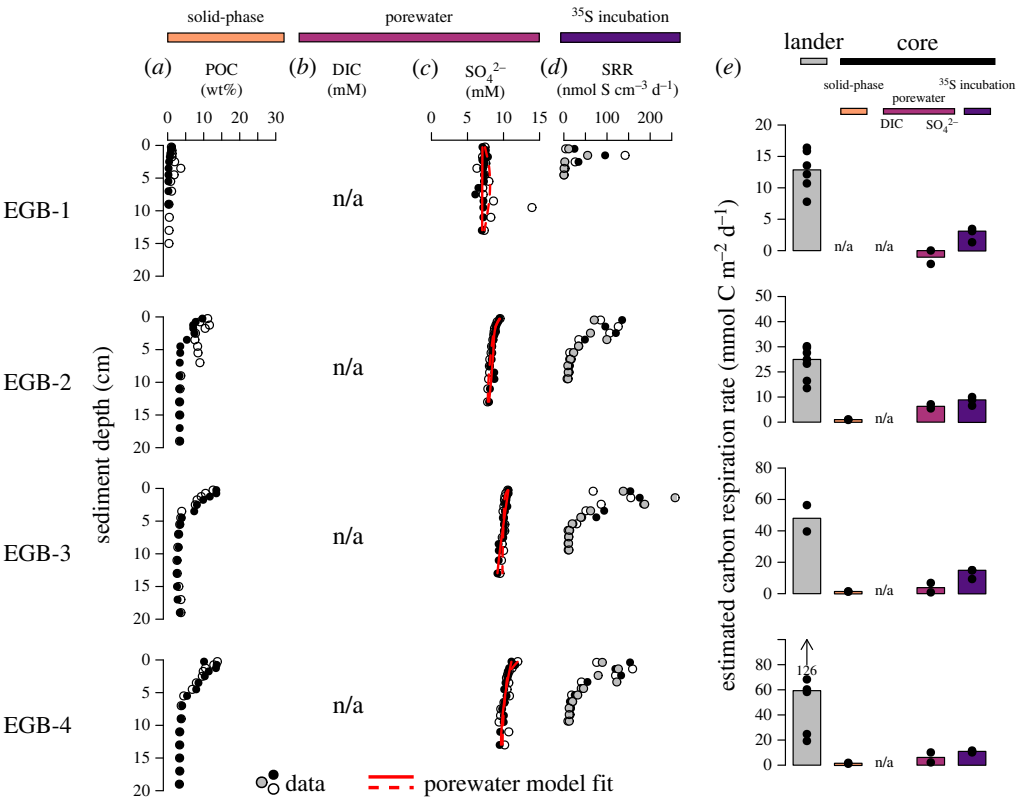

Figure 2. Results from the EGB, showing vertical sediment profiles of (*a*) POC, (*b*) DIC (not determined in the EGB sediments), (*c*) dissolved sulphate (SO_4^{2-}) and (*d*) volumetric SRR determined by the ^{35}S radiotracer method. The white, grey and black circles indicate replicate measurements. (*e*) Summary of the estimated OC respiration rates using lander-based and core-based methods. The bar height indicates the median value, points are individual measurements, and arrows and numbers indicate outliers. Note the difference in the *y*-axis for all sites. Red lines in (*b*) and (*c*) indicate diagenetic model fits used to derive production profiles with FLIPPER [40].

from approximately 13 mmol C m^{-2} d^{-1} at station EGB-1 to approximately 60 mmol C m^{-2} d^{-1} at station EGB-4 (figure 2*e*). Intriguingly, while the core-based and lander-based estimates of OC respiration show the same qualitative trend, the absolute rates estimated from cores are consistently lower than those measured *in situ* by the lander (figure 2*e*).

Data from the WGB show the same general trend as observed in the EGB sediments (figure 3). The shallow station WGB-1 contains less POC than the deeper stations (figure 3*a*), although the POC content is higher than at EGB-1. The DIC, SO_4^{2-} and SRR profiles also indicate higher respiration rates at stations WGB-2, WGB-3 and WGB-5 (figure 3*b–d*), the three deepest stations of the transect (table 1), than at station WGB-1. The *in situ* DIC fluxes follow the same pattern but indicate much higher respiration rates than those derived from the core-based methods (figure 3*e*). The only exception is station WGB-1, where the lander-derived respiration rate is comparable with the core estimates (figure 3*e*). Note however that only one chamber at WGB-1 yielded a DIC flux that is statistically significant.

4. Discussion

We estimated OC respiration rates using a lander-based *in situ* method (DIC flux) and several core-based methods (POC profile, DIC and SO_4^{2-} porewater profiles, and ^{35}S incubations). While

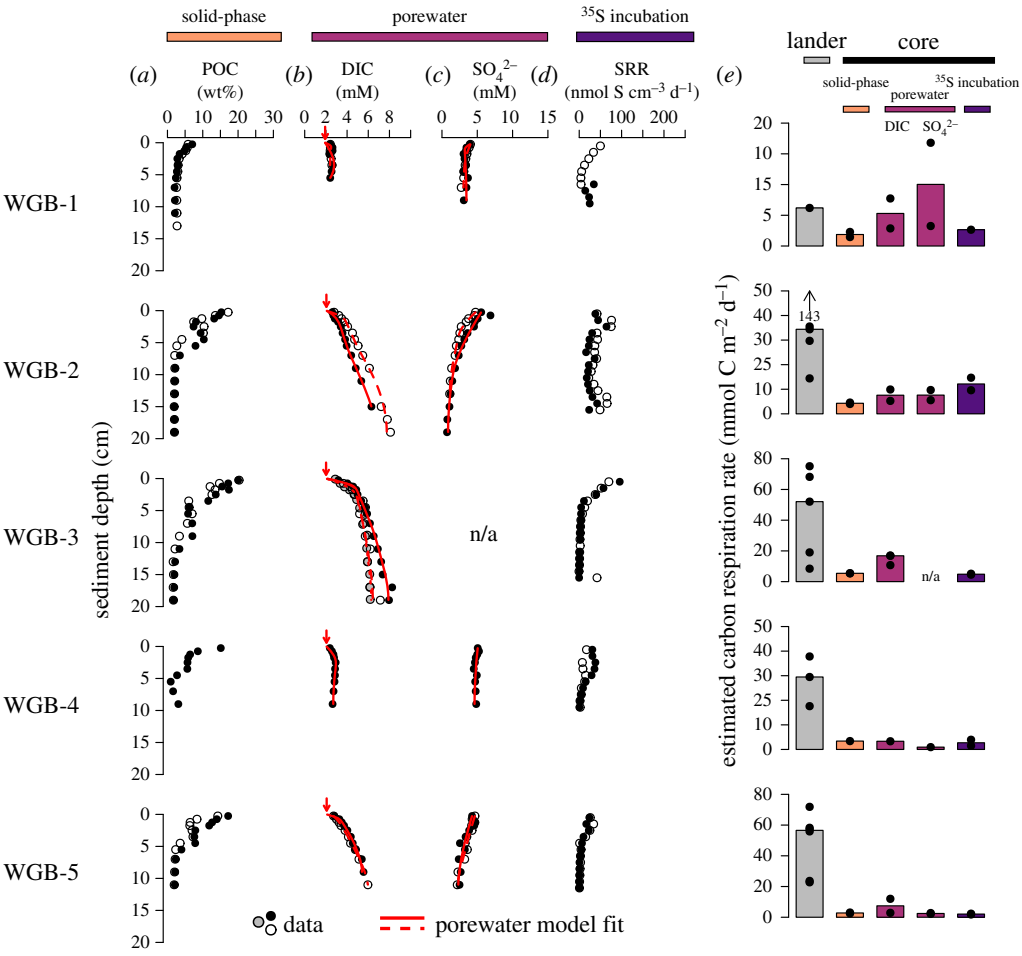

Figure 3. Results from the WGB, showing vertical sediment profiles of (*a*) POC, (*b*) DIC, (*c*) dissolved sulphate (SO_4^{2-}) and (*d*) volumetric SRR determined by the ^{35}S radiotracer method. The white, grey and black circles indicate replicate measurements. (*e*) Summary of the estimated OC respiration rate using lander-based and core-based methods. The bar height indicates the median value, points are individual measurements and arrows and numbers indicate outliers. Note the difference in the *y*-axis for all sites. Red lines in (*b*) and (*c*) indicate diagenetic model fits used to derive production profiles with FLIPPER [40]; arrows indicate bottom-water concentration.

each method has drawbacks and assumptions that may or may not be valid in our case, they should yield broadly similar results. Indeed, the core-based methods (POC, DIC, and SO_4^{2-} profiles and ^{35}S incubations) give highly similar results. The lander-based method (*in situ* DIC flux), however, suggests respiration rates that are up to an order of magnitude higher than the core-based methods (figure 4*a*).

The discrepancy between the lander-based and core-based estimates could be driven by the alteration of the DBL thickness—the layer where advective transport becomes inefficient and transport is driven mainly by diffusion—during closed chamber incubations [21]. Under steady-state conditions, the effect of the DBL thickness on the exchange of a solute is negligible [43]. However, when the DBL thickness is altered, the transient effects on the sedimentary uptake of a compound can be significant [43,44]. Altering the DBL thickness can cause the sedimentary O_2 uptake to transiently vary by approximately 30% [43,44]. Similarly, the sedimentary release of a dissolved compound (like DIC) will be affected by transient changes in DBL thickness. The water in the lander chambers is stirred to prevent chemical gradients

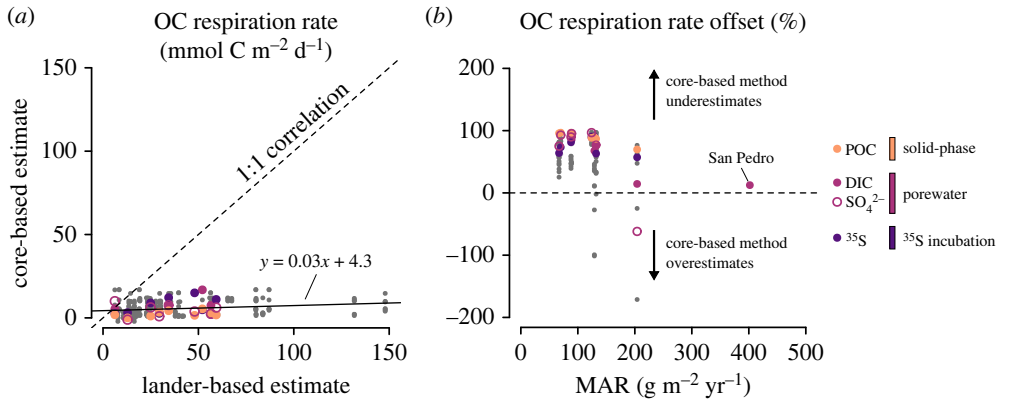

Figure 4. Difference between lander-based and core-based respiration rate estimates. (*a*) Core-based estimates of OC respiration rate versus lander-based estimates of OC respiration rates. (*b*) OC respiration rate offset (the difference between lander-base and core-based estimates, normalized against the lander-based estimate) versus MAR. Data are from this study, but also include one site from the Californian margin (San Pedro), taken from [42]. In both panels, grey dots indicate individual estimates, and coloured dots are median values.

from developing. While all care is taken to match the stirring inside the chambers to the current speed outside of the chambers [26], the DBL thickness may be altered during lander incubations. To determine the effect of DBL erosion on the lander-measured DIC flux, we used a reaction-transport model and simulated the impact of eroding a range of DBL thicknesses commonly found in marine environments. A DBL thickness of 0.2–1.0 mm is generally encountered under natural conditions [45], and DBL thicknesses of at most a few mm are measured in unmixed (and thus very stagnant) benthic chambers [44]. For the deeper part of the EGB, near-bottom current velocities are at most in the order of 2–6 cm s^{-1} [46,47], which would translate into a DBL of 0.5–1.2 mm [48]. Conditions in the WGB are very similar to the EGB, and so we assume the DBL in the WGB would be of a similar magnitude as in the EGB. If the lander completely erodes a DBL of 1.0 mm, the DIC flux can be overestimated by 8–20% throughout an incubation (figure 5). The stirring inside the landers' chambers is set at a very low speed while still maintaining homogeneity of chamber water, which means that complete erosion of the DBL is highly unlikely, and DBL erosion can thus only explain a small (less than 10%) fraction of the discrepancy between the lander-based and core-based OC respiration estimates.

The most plausible explanation for the discrepancy between the different estimates of OC respiration rates is instead that estimations from core-based methods are too low. The relative offset between lander-based and core-based methods is the smallest at the site with the highest MAR (WGB-1; figure 4*b*), suggesting that transport processes within the sediment are causing the underestimation in the core-based methods. In a sediment deposited under anoxic conditions, transport of POC away from the SWI is a result solely of slow vertical advection through sediment accumulation. By contrast, sediments deposited under (hyp)oxic conditions are often bioturbated, and POC arriving at the sediment surface is rapidly transported to the deeper sediment layers [49,50]. Even at low bottom-water O_2 concentrations (less than 20 µM), the mixed layer can be deeper than 2 cm [51]. The solid-phase and porewater gradients under anoxic conditions are thus expected to be much steeper than under (hyp)oxic conditions. The limited vertical resolution when sectioning cores will therefore lead to underestimated respiration rates in sediments underlying anoxic bottom waters, due to dilution of the highly reactive surface layer (figure 6*a*). This difference in gradient steepness between sediments underlying oxygenated and anoxic bottom water also allows us to explain the negative global correlation found between surface sediment POC concentrations and bottom-water oxygen concentrations [52] without invoking higher OC preservation in sediments with low bottom-water O_2 concentrations.

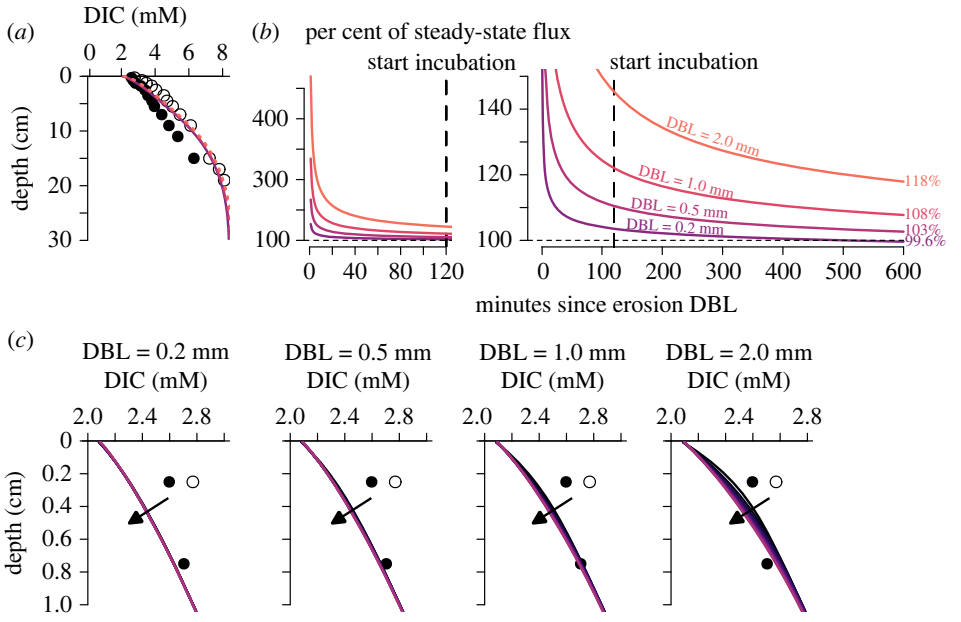

Figure 5. Impact of DBL erosion on benthic DIC fluxes. (*a*) Steady-state sediment profile of DIC for all four DBL simulation experiments. Dots are data from station WGB-2. (*b*) Temporal evolution of the instantaneous flux after complete erosion of the DBL. Note the difference in *x*-axes. The vertical dashed black line indicates the start of the actual incubation (i.e. closure of the lid—see main text for details). The value at the end of the curve indicates the value of the instantaneous flux after 10 h of incubation (relative to the steady-state flux). (*c*) Evolution of the DIC profile near the sediment-water interface during the incubation. The arrow indicates the direction of change.

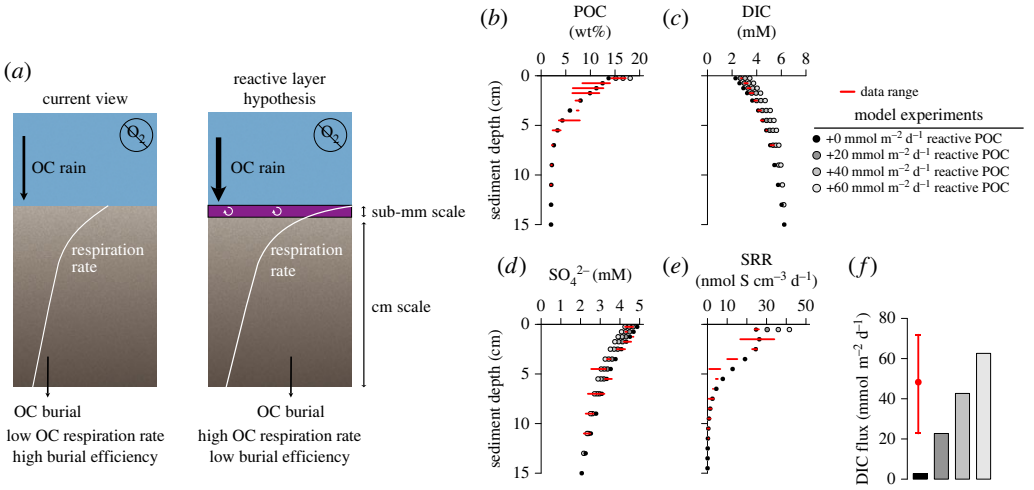

Figure 6. Reaction-transport model experiments illustrating the impact of the reactive surface layer. (*a*) The reactive surface layer hypothesis, see text for details. (*b–f*) Impact of adding POC with a degradation constant of 10 year^{-1} on down-core profiles of (*b*) POC, (*c*) DIC, (*d*) dissolved sulphate (SO_4^{2-}) and (*e*) SRR, as well as (*f*) the benthic DIC fluxes. For the modelled down-core profile of SRR, it was assumed that the first 0.5 mm sediment surface layer was not accurately captured during the incubation, and the first modelled point represents the 0.05–1.0 cm interval (see text for details). Data are from station WGB-5. Model details and parameters can be found in the electronic supplementary material, text, section S2.

To test our reactive layer hypothesis, we set up a one-dimensional reaction-transport model and calibrated it to the site where the difference between lander-based and core-based respiration rates was the largest, and for which we have the most complete dataset (WGB-5; figure 3).

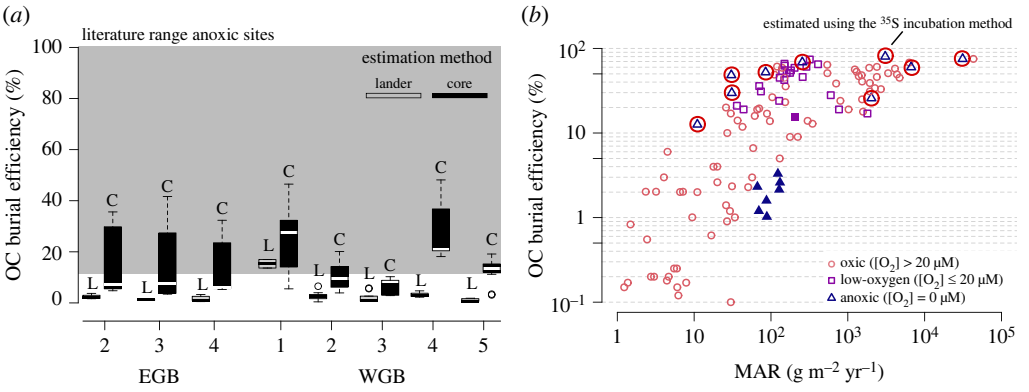

Figure 7. (*a*) The comparison of OC burial efficiencies for each field site of this study calculated using the lander-based method (grey boxplots, indicated with an L) and the different core-based methods (black boxplots, indicated with a C). The literature range (grey-shaded area) of burial efficiencies in anoxic environments is taken from [4]. (*b*) Literature compilation of OC burial efficiencies versus MAR, reproduced from refs [4,5], with the inclusion of new data [19,20,58–63] (data are summarized in the electronic supplementary material, table S2). Filled symbols are lander-based OC burial efficiencies from this study. OC burial efficiencies from the literature derived from ^{35}S incubations are indicated by the red circles around the empty triangles.

When calibrating the model to the core-based data, we were able to reproduce the observed profiles (figure 6*b–e*) but underestimated the lander-measured DIC flux by more than an order of magnitude (2.5 versus 23–72 mmol C m^{-2} d^{-1}; figure 6*f*). When we subsequently added an influx of highly reactive OC with a reactivity constant of 10 yr^{-1}, which is representative for highly reactive marine OC [53], the change in down-core profiles was limited, but the simulated DIC flux fell within the measured range (figure 6*b–f*). We only found a major impact on the SRR near the SWI, with simulated rates of 1–3 µmol S cm^{-3} d^{-1} in the first centimetre (two orders of magnitude higher than the measured SRR). However, when the top 0.5 mm was excluded, the surface simulated rates were comparable with the measured SRR (figure 6*e*). Several manipulations during the ^{35}S incubation are likely to reduce the SRR in the top 0.5 mm, such as the removal of the overlying water or potential oxidation artefacts during incubation (which were not kept in an anoxic atmosphere). In summary, our model experiment shows that the majority of OC respiration can occur in the upper 0.5 mm below the SWI, or directly at the SWI, without having a major influence on the down-core profiles. Hence, the use of core-based profiles to derive OC respiration rates can underestimate the actual OC respiration rate substantially in unbioturbated settings such as in anoxic environments. Since around 15% of the coastal ocean has a negligible mixed layer [54], we propose that the reactive surface layer is an important feature in the global coastal seafloor.

The predominant use of core-based methods when estimating OC respiration rates in sediments underlying anoxic bottom waters [5,17] has led to the global impact of bottom-water anoxia on OC burial efficiencies being overestimated. Other studies comparing lander-based OC respiration rate estimates with core-based estimates at unbioturbated sites are rare, yet the literature supports our interpretation [55–57]. Higher phosphate fluxes—a possible proxy for OC respiration—have been measured in chamber incubations than calculated from sediment profiles in unbioturbated sediments underlying hypoxic or anoxic bottom waters in the Peruvian oxygen-minimum zone (lander-based estimates were 50–210% higher; [55]) and the Pakistan margin oxygen-minimum zone (lander-based estimates were orders of magnitude higher; [56]). Additionally, a recent study in the hypoxic Gulf of Mexico estimated a seven times higher respiration rate based on high-resolution oxygen microsensor profiles compared with core-based DIC profiles [57]. Because of the higher vertical advective velocity at higher MARs, the respiration rate offsets are expected to decrease with increasing MARs. The offset between core-based and lander-based OC respiration rate estimates is indeed small at our site with the highest MAR (WGB-1). Observations from the unbioturbated southern California borderland basins also show

a negligible offset in respiration rate estimates in San Pedro, a basin with high MAR (approx. 400 $g\,m^{-2}\,yr^{-1}$) [42] (figure 4*b*).

The methodological artefacts in estimating OC respiration rates translate into a substantial difference between calculated OC burial efficiencies (figures 6*a* and 7*a*). Using the core-based estimate, we obtain burial efficiency values in line with previous estimates for OC burial efficiencies in sediments underlying anoxic water columns (5–50%, median: 8.4%) [4]. When we use the lander-based estimates, however, the OC burial efficiencies become substantially lower, of the order of 0.5–15% (median: 1.2%), contrary to existing literature (figure 7*a*; [4,7]). Therefore, we propose that the apparent difference in OC burial efficiencies for sediments deposited in oxic versus anoxic conditions in the literature is caused by methodological artefacts. Indeed, when we omit the OC burial efficiencies that have been calculated based on core-based methods alone and include our new lander-based estimates (figure 7*b*), we draw the following conclusions: (i) the OC in the anoxic Baltic Sea sediments is more reactive than expected compared with oxygenated sediments with similar MARs and (ii) there is no clear influence of bottom-water O_2 conditions on OC burial efficiency.

5. Conclusion

We demonstrate that a reactive surface layer of submillimetre scale, which accounts for greater than 50% of the respiration rate of the entire sediment column, exists in sediments without a mixed layer. By not accounting for the presence of this reactive surface layer, the OC burial efficiency can be overestimated by a factor of 10. Around 15% of the modern coastal seafloor does not have a mixed layer [54]. In these regions, respiration rates, and thus OC rain rates, are likely underestimated. Our findings are especially pertinent in the context of past O_2-poor oceans. A limited impact of oxygen on OC burial efficiency provides support for the hypothesis that aerobic respiration drove Earth's oxygenation [64]. Additionally, our results question the assumption of enhanced OC burial efficiency in a seafloor underlying anoxic bottom waters, which is used in recent reconstructions of marine primary productivity during periods of extensive ocean anoxia in the Cretaceous, the Proterozoic and Archean Eon [65,66]. These studies suggest marine primary productivities that were 100 times (for the Proterozoic) to 1000 times (for the Archean) lower than today, mainly because of the assumption of enhanced OC burial efficiencies in anoxic oceans [66]. Our results and re-interpretation of literature data show that water-column O_2 concentrations are not a major factor controlling OC burial (figure 7*b*) and that OC burial efficiencies are likely overestimated by an order of magnitude (figure 4*a*). As a result, the difference in oxygenation in the deep ocean in the past would have had little impact on OC burial, and primary production rates in the past oceans were likely 10 times higher than currently assumed.

Data accessibility. The data are provided in the electronic supplementary material [67].

Authors' contributions. S.J.V.: conceptualization, formal analysis, investigation, methodology, writing—original draft and writing—review and editing; A.H.: investigation, methodology and writing—review and editing; M.E.: investigation and writing—review and editing; R.K.J.: investigation and writing—review and editing; M.Y.K.: investigation, methodology and writing—review and editing; E.K.R.: investigation and writing—review and editing; P.O.J.H.: funding acquisition, investigation, methodology and writing—review and editing.

All authors gave final approval for publication and agreed to be held accountable for the work performed therein.

Conflict of interest declaration. The authors declare they have no competing interests.

Funding. The research leading to this manuscript was supported by grants from the Swedish Research Council (grant no. 2015-03717 to P.O.J.H.), the Swedish Agency for Marine and Water Management (grant no. 2535-20 to P.O.J.H.) and the Belgian Federal Science Policy Office (grant nos. FED-tWIN2019-prf-008, RV/21/CANOE and RV/21/DEHEAT to S.J.V.). R.K.J. is a postdoctoral fellow from the Fonds de la Recherche Scientifique.

Acknowledgements. The authors would like to thank the crew of the University of Gothenburg RV Skagerak for technical assistance, Marie Karlsson at Linköping University for her assistance in the polonium analysis of the

^{210}Pb samples, Heidi Grøn Jensen for assistance during the ^{35}S incubations and extractions, and Bo Thamdrup for comments on an earlier version of the manuscript.

References

1. Berner RA. 1982 Burial of organic carbon and pyrite sulfur in the modern ocean: its geochemical and environmental sinificance. *Am. J. Sci.* **282**, 451–473. (doi:10.2475/ajs.282.4.451)
2. Hedges JI, Keil RG. 1995 Sedimentary organic matter preservation: an assessment and speculative synthesis. *Mar. Chem.* **49**, 81–115. (doi:10.1016/0304-4203(95)00008-F)
3. Arndt S, Jørgensen BB, LaRowe DE, Middelburg JJ, Pancost RD, Regnier P. 2013 Quantifying the degradation of organic matter in marine sediments: a review and synthesis. *Earth Sci. Rev.* **123**, 53–86. (doi:10.1016/J.EARSCIREV.2013.02.008)
4. Canfield DE. 1994 Factors influencing organic carbon preservation in marine sediments. *Chem. Geol.* **114**, 315–329. (doi:10.1016/0009-2541(94)90061-2)
5. Burdige DJ. 2007 Preservation of organic matter in marine sediments: controls, mechanisms, and an imbalance in sediment carbon budgets? *Chem. Rev.* **107**, 467–485. (doi:10.1021/cr050347q)
6. Hartnett HE, Keil RG, Hedges JI, Devol AH. 1998 Influence of oxygen exposure time on organic carbon preservation in continental margin sediments. *Nature* **391**, 572–574. (doi:10.1038/35351)
7. Katsev S, Crowe SA. 2015 Organic carbon burial efficiencies in sediments: the power law of mineralization revisited. *Geology* **43**, 607–610. (doi:10.1130/G36626.1)
8. Shang H. 2023 A generic hierarchical model of organic matter degradation and preservation in aquatic systems. *Commun. Earth Environ.* **4**, 16. (doi:10.1038/s43247-022-00667-4)
9. Moodley L, Middelburg JJ, Herman PMJ, Soetaert K, de Lange GJ. 2005 Oxygenation and organic-matter preservation in marine sediments: direct experimental evidence from ancient organic carbon-rich deposits. *Geology* **33**, 889. (doi:10.1130/G21731.1)
10. Kristensen E, Ahmed SI, Devol AH. 1995 Aerobic and anaerobic decomposition of organic matter in marine sediment: which is fastest? *Limnol. Oceanogr.* **40**, 1430–1437. (doi:10.4319/lo.1995.40.8.1430)
11. Hulthe G, Hulth S, Hall POJ. 1998 Effect of oxygen on degradation rate of refractory and labile organic matter in continental margin sediments. *Geochim. et Cosmochim. Acta.* **62**, 1319–1328. (doi:10.1016/S0016-7037(98)00044-1)
12. LaRowe DE, Van Cappellen P. 2011 Degradation of natural organic matter: a thermodynamic analysis. *Geochim. Cosmochim. Acta* **75**, 2030–2042. (doi:10.1016/J.GCA.2011.01.020)
13. Emerson S, Hedges JI. 1988 Processes controlling the organic carbon content of open ocean sediments. *Palaeoceanography* **3**, 621–634. (doi:10.1029/PA003i005p00621)
14. Woulds C *et al.* 2007 Oxygen as a control on sea floor biological communities and their roles in sedimentary carbon cycling. *Limnol. Oceanogr.* **52**, 1698–1709. (doi:10.4319/LO.2007.52.4.1698)
15. Middelburg JJ, Levin LA. 2009 Coastal hypoxia and sediment biogeochemistry. *Biogeosciences* **6**, 1273–1293. (doi:10.5194/bg-6-1273-2009)
16. Helly JJ, Levin LA. 2004 Global distribution of naturally occurring marine hypoxia on continental margins. *Deep Sea Res. 1 Oceanogr. Res. Pap.* **51**, 1159–1168. (doi:10.1016/j.dsr.2004.03.009)
17. Canfield DE. 1989 Sulfate reduction and oxic respiration in marine sediments: implications for organic carbon preservation in euxinic environments. *Deep-Sea Res.* **36**, 121–138. (doi:10.1016/0198-0149(89)90022-8)
18. Glud RN. 2008 Oxygen dynamics of marine sediments. *Mar. Biol. Res.* **4**, 243–289. (doi:10.1080/17451000801888726)
19. Dale AW *et al.* 2015 Organic carbon production, mineralisation and preservation on the Peruvian margin. *Biogeosciences* **12**, 1537–1559. (doi:10.5194/bg-12-1537-2015)
20. Berelson WM, McManus J, Coale KH, Johnson KS, Kilgore T, Burdige D, Pilskaln C. 1996 Biogenic matter diagenesis on the sea floor: a comparison between two continental margin transects. *J. Mar. Res.* **54**, 731–762. (doi:10.1357/0022240963213673)
21. Santschi P, Höhener P, Benoit G, Buchholtz-ten Brink M. 1990 Chemical processes at the sediment-water interface. *Mar. Chem.* **30**, 269–315. (doi:10.1016/0304-4203(90)90076-O)
22. Jahnke RA. 1990 Early diagenesis and recycling of biogenic debris at the seafloor, Santa Monica Basin, California. *J. Mar. Res.* **48**, 413–436. (doi:10.1357/002224090784988773)

23. Nilsson MM, Hylén A, Ekeroth N, Kononets MY, Viktorsson L, Almroth-Rosell E, Roos P, Tengberg A, Hall POJ. 2021 Particle shuttling and oxidation capacity of sedimentary organic carbon on the Baltic Sea system scale. *Mar. Chem.* **232**, 103963. (doi:10.1016/J.MARCHEM.2021.103963)
24. Nilsson M *et al.* 2018 Organic carbon recycling in Baltic Sea sediments - An integrated estimate on the system scale based on *in situ* measurements. *Mar. Chem.* **209**, 81–93. (doi:10.1016/j.marchem.2018.11.004)
25. Carman R, Cederwall H. 2001 Sediments and Macrofauna in the Baltic Sea — characteristics, nutrient contents and distribution. In *Ecological studies*, pp. 289–327. Berlin, Germany: Springer.
26. Kononets M, Nilsson M, Tengberg A, Ekeroth N, Hylén A, van de Velde S, Blomqvist S, Hall POJ. 2021 In situ incubations with the Gothenburg benthic chamber landers: applications and quality control. *J. Mar. Sys.* **214**, 103475. (doi:10.1016/j.jmarsys.2020.103475)
27. Tengberg A, Ståhl H, Gust G, Müller V, Arning U, Andersson HJ, Hall POJ. 2004 Intercalibration of benthic flux chambers I. Accuracy of flux measurements and influence of chamber hydrodynamics. *Prog. Oceanogr.* **60**, 1–28. (doi:10.1016/j.pocean.2003.12.001)
28. van de Velde SJ, Hylén A, Kononets M, Marzocchi U, Leermakers M, Choumiline K, Hall POJ, Meysman FJR. 2020 Elevated sedimentary removal of Fe, Mn, and trace elements following a transient oxygenation event in the Eastern Gotland Basin, central Baltic Sea. *Geochim. Cosmochim. Acta* **271**, 16–32. (doi:10.1016/j.gca.2019.11.034)
29. Blomqvist S, Ekeroth N, Elmgren R, Hall P. 2015 Long overdue improvement of box corer sampling. *Mar. Ecol. Prog. Ser.* **538**, 13–21. (doi:10.3354/meps11405)
30. Appleby PG, Oldfield F. 1978 The calculation of lead-210 dates assuming a constant rate of supply of unsupported 210Pb to the sediment. *Catena (Amst)* **5**, 1–8. (doi:10.1016/S0341-8162(78)80002-2)
31. Sanchez-Cabeza JA, Ani-Ragolta I, Masquè P. 2000 Some considerations of the ^{210}Pb constant rate of supply (CRS) dating model. *Limnol. Oceanogr.* **45**, 990–995. (doi:10.4319/lo.2000.45.4.0990)
32. Flynn WW. 1968 The determination of low levels of polonium-210 in environmental materials. *Anal. Chim. Acta* **43**, 221–227. (doi:10.1016/S0003-2670(00)89210-7)
33. Ehinger SC, Pacer RA, Romines FL. 2005 Separation of the radioelements ^{210}Pb–^{210}Bi–^{210}Po by spontaneous deposition onto noble metals and verification by Cherenkov and liquid scintillation counting. *J. Radioanal. Nucl. Chem.* **98**, 39–48. (doi:10.1007/BF02060431)
34. Henricsson F, Ranebo Y, Holm E, Roos P. 2011 Aspects on the analysis of ^{210}Po. *J. Environ. Radioact.* **102**, 415–419. (doi:10.1016/J.JENVRAD.2010.09.010)
35. Mauring A, Gäfvert T. 2013 Radon tightness of different sample sealing methods for gamma spectrometric measurements of ^{226}Ra. *Appl. Radiat. Isot.* **81**, 92–95. (doi:10.1016/J.APRADISO.2013.03.022)
36. Jørgensen BB. 1978 A comparison of methods for the quantification of bacterial sulfate reduction in coastal marine sediments: I. measurement with radiotracer techniques. *Geomicrobiol. J.* **1**, 11–27. (doi:10.1080/01490457809377721)
37. Canfield DE, Raiswell R, Westrich JT, Reaves CM, Berner RA. 1986 The use of chromium reduction in the analysis of reduced inorganic sulfur in sediments and shales. *Chem. Geol.* **54**, 149–155. (doi:10.1016/0009-2541(86)90078-1)
38. Gros N, Camões MF, Oliveira C, Silva MCR. 2008 Ionic composition of seawaters and derived saline solutions determined by ion chromatography and its relation to other water quality parameters. *J. Chromatogr. A* **1210**, 92–98. (doi:10.1016/j.chroma.2008.09.046)
39. Thamdrup B, Canfield DE. 1996 Pathways of carbon oxidation in continental margin sediments off central Chile. *Limnol. Oceanogr.* **41**, 1629–1650. (doi:10.4319/lo.1996.41.8.1629)
40. van de Velde SJ, Burdorf LDW, Meysman FJR. 2022 Code for: FLIPPER - flexible interpretation of porewater profiles and estimation of rates. *Zenodo*. (doi:10.5281/zenodo.662498)
41. Berg P, Risgaard-petersen N, Silkeborg D. 1998 Interpretation of measured concentration profiles in sediment pore water. *Limnol. Oceanogr.* **43**, 1500–1510. (doi:10.4319/lo.1998.43.7.1500)
42. Berelson WM, Hammond DE, Johnson KS. 1987 Benthic fluxes and the cycling of biogenic silica and carbon in two southern California borderland basins. *Geochim. Cosmochim. Acta* **51**, 1345–1363. (doi:10.1016/0016-7037(87)90320-6)

43. Glud RN, Berg P, Fossing H, Jørgensen BB. 2007 Effect of the diffusive boundary layer on benthic mineralization and O_2 distribution: a theoretical model analysis. *Limnol. Oceanogr.* **52**, 547–557. (doi:10.4319/LO.2007.52.2.0547)
44. Hall POJ, Anderson LG, van der Loeff MMR, Sundby B, Westerlund SFG. 1989 Oxygen uptake kinetics in the benthic boundary layer. *Limnol. Oceanogr.* **34**, 734–746. (doi:10.4319/LO.1989.34.4.0734)
45. Jørgensen BB, Revsbech NP. 1985 Diffusive boundary layers and the oxygen uptake of sediments and detritus. *Limnol. Oceanogr.* **30**, 111–122. (doi:10.4319/lo.1985.30.1.0111)
46. Hille S, Leipe T, Seifert T. 2006 Spatial variability of recent sedimentation rates in the Eastern Gotland Basin (Baltic Sea). *Oceanologia* **48**, 287–307.
47. Christiansen C, Kunzendorf H, Emeis K, Endler R, Struck U, Neumann T, Sivkov V. 2002 Temporal and spatial sedimentation rate variabilities in the Eastern Gotland Basin, the Baltic Sea. *Boreas* **31**, 65–74. (doi:10.1111/j.1502-3885.2002.tb01056.x)
48. Santschi PH, Anderson RF, Fleisher MQ, Bowles W. 1991 Measurements of diffusive sublayer thicknesses in the ocean by alabaster dissolution, and their implications for the measurements of benthic fluxes. *J. Geophys. Res. Oceans* **96**, 10 641–10 657. (doi:10.1029/91JC00488)
49. Berner RA, Westrich JT. 1985 Bioturbation and the early diagenesis of carbon and sulfur. *Am. J. Sci.* **285**, 193–206. (doi:10.2475/ajs.285.3.193)
50. Aller RC, Cochran JK. 2019 The critical role of bioturbation for particle dynamics, priming potential, and organic C remineralization in marine sediments: local and basin scales. *Front. Earth Sci. (Lausanne)* **7**, 1–14. (doi:10.3389/feart.2019.00157)
51. Smith CR, Levin LA, Hoover DJ, McMurtry G, Gage JD. 2000 Variations in bioturbation across the oxygen minimum zone in the northwest Arabian Sea. *Deep Sea Res. 2 Top Stud. Oceanogr.* **47**, 227–257. (doi:10.1016/S0967-0645(99)00108-3)
52. Bianchi TS, Schreiner KM, Smith RW, Burdige DJ, Woodard S, Conley DJ. 2016 Redox effects on organic matter storage in coastal sediments during the Holocene: a BiomarkerProxy perspective. *Annu. Rev. Earth Planet Sci.* **44**, 295–319. (doi:10.1146/annurev-earth-060614-105417)
53. Westrich JT, Berner RA. 1984 The role of sedimentary organic matter in bacterial sulfate reduction: the G model tested. *Limnol. Oceanogr.* **29**, 236–249. (doi:10.4319/lo.1984.29.2.0236)
54. Song S *et al.* 2023 A global assessment of the mixed layer in coastal sediments and implications for carbon storage. *Nat. Commun.* **13**, 4903. (doi:10.1038/s41467-022-32650-0)
55. Noffke A, Hensen C, Sommer S, Scholz F, Bohlen L, Mosch T, Graco M, Wallmann K. 2012 Benthic iron and phosphorus fluxes across the Peruvian oxygen minimum zone. *Limnol. Oceanogr.* **57**, 851–867. (doi:10.4319/lo.2012.57.3.0851)
56. Woulds C, Schwartz MC, Brand T, Cowie GL, Law G, Mowbray SR. 2009 Porewater nutrient concentrations and benthic nutrient fluxes across the Pakistan margin OMZ. *Deep Sea Res. Part II* **56**, 333–346. (doi:10.1016/J.DSR2.2008.05.034)
57. Rabouille C *et al.* 2021 Early diagenesis in the hypoxic and acidified zone of the Northern Gulf of Mexico: is organic matter recycling in sediments disconnected from the water column? *Front. Mar. Sci.* **8**, 1–18. (doi:10.3389/fmars.2021.604330)
58. Ståhl H, Hall POJ, Tengberg A, Josefson AB, Streftaris N, Zenetos A, Karageorgis AP. 2004 Respiration and sequestering of organic carbon in shelf sediments of the oligotrophic northern Aegean Sea. *Mar. Ecol. Prog. Ser.* **269**, 33–48. (doi:10.3354/meps269033)
59. Ståhl H, Tengberg A, Brunnegård J, Hall POJ. 2004 Recycling and burial of organic carbon in sediments of the Porcupine Abyssal Plain, NE Atlantic. *Deep Sea Res. 1 Oceanogr. Res. Pap.* **51**, 777–791. (doi:10.1016/j.dsr.2004.02.007)
60. Hulth S, Tengberg A, Landén A, Hall POJ. 1997 Mineralization and burial of organic carbon in sediments of the southern Weddell Sea (Antarctica). *Deep Sea Res. 1 Oceanogr. Res. Pap.* **44**, 955–981. (doi:10.1016/S0967-0637(96)00114-8)
61. Glud RN, Holby O, Hoffmann F, Canfield DE. 1998 Benthic mineralization and exchange in Arctic sediments (Svalbard, Norway). *Mar. Ecol. Prog. Ser.* **173**, 237–251. (doi:10.3354/meps173237)
62. Berelson W *et al.* 2003 A time series of benthic flux measurements from Monterey Bay, CA. *Cont. Shelf Res.* **23**, 457–481. (doi:10.1016/S0278-4343(03)00009-8)
63. Oueslati W, van de Velde S, Helali MA, Added A, Aleya L, Meysman FJR. 2019 Carbon, iron and sulphur cycling in the sediments of a Mediterranean lagoon (Ghar El Melh, Tunisia). *Estuar. Coast Shelf Sci.* **221**, 156–169. (doi:10.1016/j.ecss.2019.03.008)

64. Shang H, Rothman DH, Fournier GP. 2022 Oxidative metabolisms catalyzed Earth's oxygenation. *Nat. Commun.* **13**, 1328. (doi:10.1038/s41467-022-28996-0)
65. Bauer KW, McKenzie NR, Bottini C, Erba E, Crowe SA. 2022 Carbon pump dynamics and limited organic carbon burial during OAE1a. *Geobiology* **21**, 341–354. (doi:10.1111/gbi.12538)
66. Planavsky NJ, Fakhraee M, Bolton EW, Reinhard CT, Isson TT, Zhang S, Mills BJW. 2022 On carbon burial and net primary production through Earths history. *Am. J. Sci.* **322**, 413–460. (doi:10.2475/03.2022.01)
67. van de Velde SJ, Hylén A, Eriksson M, James RK, Kononets MY, Robertson EK, Hall POJ. 2023 Exceptionally high respiration rates in the reactive surface layer of sediments underlying oxygen-deficient bottom waters. Figshare. (doi:10.6084/m9.figshare.c.6729334)